Available online at www.sciencedirect.com
SCIENCE DIRECT®
Electric Power Systems Research 73 (2005) 217–226
ELECTRIC POWER SYSTEMS RESEARCH
www.elsevier.com/locate/epsr

Weakest bus, most loaded transmission path and critical branch identification for voltage security reinforcement

R.B. Prada[a,*], E.G.C. Palomino[a], L.A.S. Pilotto[b], A. Bianco[b]

[a] *Department of Electrical Engineering, Catholic University, Rio de Janeiro, Rua Marques de Sao Vicente 225, Gavea, RJ 22453 900, Brazil*
[b] *CEPEL, Electric Power Research Centre, Rio de Janeiro 21941 590, Brazil*

Received 28 May 2003; accepted 16 August 2004
Available online 14 November 2004

Abstract

Maximum power transmission and inadequate voltage control are the two main aspects associated with voltage security analysis. Once weak buses are found by the assessment function, enhancement control actions be may recommended. This paper presents a sequential iterative method to reinforce system conditions. A simple illustrative 34-bus system is used to show the adequacy and efficiency of the power flow reduction through the "critical branch" of the "most loaded transmission path". Both concepts are introduced in this paper.

Keywords: Voltage security; Voltage control; Voltage stability; Voltage collapse; Power flow

1. Introduction

Voltage stability analysis, or more adequately, voltage security analysis, may be divided in two aspects: the assessment function and, if necessary, the reinforcement function. The voltage security assessment may find results of two different types: (i) the power flow arriving in a load bus is reaching its maximum, (ii) the effect of voltage-control actions in a voltage-controlled bus may be opposite to the expected one [1,2].

The objective of the voltage security assessment is to point out the weakest buses for the operating point under analysis. The concept of weakest bus, i.e. the critical bus from the voltage security point of view, is fully described in [3]. Once the assessment is performed, the objective of the reinforcement function is to calculate adequate control actions in order to increase the "distance" between the actual load and the (new) maximum power flow. Several times this may be achieved by voltage profile changes and consequent loss reduction. Sometimes that procedure is not enough and active generation rescheduling is recommended.

A load bus may receive active power from different transmission paths. Consider, for instance, two generators connected to one load through two different transmission lines. Suppose that all load increase is supplied by only one of the two generators and thus increasing the power flow across the corresponding transmission line. As the load continues to increase, the power flow that can be transmitted to the load reaches its maximum. It is obvious that the load may continue to increase, provided the idle generator starts providing the necessary power and thus loading the other transmission line.

The intention is, therefore, to determine the different routes being used for active power flow transmission to the weakest load bus, to identify the most loaded transmission path, and redirect the power flow to other routes less loaded. The initial option is to do that by voltage profile adjustment and, if necessary, by active power rescheduling.

* Corresponding author. Tel.: +55 21 31141214; fax: +55 21 31141232.
E-mail addresses: edgardo@ufba.br (E.G.C. Palomino), luis.pilotto@andradecanellas.com.br (L.A.S. Pilotto), Andre.Bianco@andradecanellas.com.br (A. Bianco).

0378-7796/$ – see front matter © 2004 Elsevier B.V. All rights reserved.
doi:10.1016/j.epsr.2004.08.006

2. Most loaded transmission path and critical branch

2.1. Subnetwork identification

The first procedure is to identify the part of the full network that is actually being used for active power flow transmission to the weakest load bus, as well as the corresponding generators. The following steps are necessary:

(1) The sign of the active power flow is used to establish the subnetwork as follows. Buses j connected to the weakest bus i belong to the subnetwork if $P_{ij} < 0$, where P_{ij} is the active power leaving bus i in the direction of bus j. Buses k connected to buses j belong to the subnetwork if $P_{jk} < 0$. Buses l connected to buses k belong to the subnetwork if $P_{kl} < 0$. The search continues on other bus layers until a generation bus is found. The subnetwork is established. Although not as simple, an alternative for this step is the "downstream-looking" algorithm [4].
(2) In order to isolate the subnetwork from the remaining network, it is necessary to convert the active power flows leaving the subnetwork from intermediate buses, as well as the reactive power flows leaving and arriving the intermediate buses of the subnetwork into admittances. Note that, by definition, there are no active powers being injected into intermediate buses of the subnetwork. The system now has reduced dimension and comprises one load bus connected by a network with intermediate nodes to one or more generators.

2.2. Transmission paths identification

The second procedure is to identify radial transmission paths between the load bus and each generator, and eliminate intermediate nodes. The following steps are necessary:

(1) Each bus j connected by a transmission branch to the weakest load bus i defines one radial transmission path. Note that $P_{ij} < 0$. If there are nj buses j, nj paths are defined. For each bus j there are nk buses k connected to them with $P_{jk} < 0$ and $nk - 1$ new paths are defined. For each bus k, there are nl buses l connected to them with $P_{kl} < 0$ and $nl - 1$ new paths are defined. The search continues on other bus layers until a generation bus is found. Each path finishes at a generator m.
Therefore, several radial transmission paths are defined and each of them includes the weakest bus i, several intermediate buses such as bus j, bus k, bus l, and a generator bus m. These transmission paths are not necessarily independent; the same transmission branch may belong to more than one path, as well as the same generator may appear in more than one path.
(2) In order to seclude the radial transmission path from the remaining part of the subnetwork, it is necessary to convert all active and reactive power flows leaving and arriving the path at intermediate nodes into admittances.
(3) Transforming loads of the intermediate buses into admittances and eliminating these nodes by "network reduction" [5], an equivalent 2-bus system is obtained. Network reduction was a common practice in angular stability analysis by time domain simulation [6].

Several 2-bus systems, comprising one generator, one load, and one π-equivalent transmission circuit, are obtained. The same generator may be connected to the load bus through different π-equivalent circuits. The individuality of each parallel transmission path is maintained.

The load of each 2-bus system is the active and reactive power flow that arrives at the load bus through the corresponding path. Similarly, the generation of each 2-bus system is the active and reactive power that leaves the generator bus through the corresponding path.

The variables that have the same value in the full network and in the reduced 2-bus system are voltage angle and magnitude both in the generator and in the load, the generation, i.e. the power flow entering the 2-bus system, and the load, i.e. the power flow leaving the 2-bus system.

The reduced π-equivalent transmission circuits depend on the network admittance and also on the nodal voltages because power flows are converted into admittances. Therefore, the reduced π-equivalent transmission circuits are valid only for the operating point under analysis and, at the most, for infinitesimal variations.

The series and shunt branches of the reduced π-equivalent transmission circuit are not necessarily similar to those of a transmission line. However, the interest lies on verifying the "transmission effort", i.e. the voltage magnitude drop and the voltage angle displacement, which is the same when measured using the full network and the 2-bus system.

2.3. Most loaded transmission path recognition

The third procedure is the comparison between the load voltage of the operating point under analysis and the critical voltage, which is the one when load is at the maximum. The critical voltage magnitude and angle are calculated by the formulas of V_l^c and θ_l^c stated below. With the comparison, it is possible to determine whether the load voltage is on the upper or on the lower half of the well-known $V \times P$ curve, with constant power factor, as well as the "distance" to the critical voltage at the maximum load. The most loaded transmission path is the one which presents the smallest "distance" between the load voltage of the operating point under analysis and the critical one. Unmistakably, the comparison result is valid only for the operating point under analysis.

For a 2-bus system, comprising one generator, one load, and one π-equivalent transmission circuit, it is known that [1]:

$$\theta_l^c = \frac{1}{2} \times \text{arc tg} \times \left(\frac{\sin(-\phi + \alpha_t) + (Z_t/Z_s)\sin(-\phi + 2\alpha_t - \alpha_s)}{-\cos(-\phi + \alpha_t) - (Z_t/Z_s)\cos(-\phi + 2\alpha_t - \alpha_s)} \right) + \theta_g$$

$$V_l^c = \frac{V_g}{2\cos(\theta_l^c - \theta_g) + 2(Z_t/Z_s)\cos(\theta_l^c - \theta_g + \alpha_t - \alpha_s)}$$

where V_l^c, θ_l^c are the load voltage magnitude and angle when load is at the maximum, V_g, θ_g the generator voltage magnitude and angle, Z_t, α_t the π-equivalent circuit series branch impedance magnitude and angle, Z_s, α_s the π-equivalent circuit shunt branch impedance magnitude and angle (load side), ϕ is the load power factor angle.

2.4. Critical branch identification

The fourth procedure is to analytically recognise the critical branch of the most loaded transmission path, i.e. the branch to have its flow decreased. The idea is to examine the first path including the generator m and the branch $m-l$. The voltage at the bus l is compared with the critical one corresponding to the maximum power flow arriving at this bus. Following the analysis, a new branch $l-k$ is included and, consequently, the second path is from bus m to bus l and to bus k. Again, the voltage at the bus k is compared with the critical one. New branches are included sequentially until the load bus i is reached. The critical branch is the one that, when included, presents the smallest "distance" between the load voltage and the critical one. The following numerical example clarifies the procedures described in this section.

3. Numerical example

The aim is to identify the weakest bus from the voltage security point of view, the most loaded transmission path for that bus, again from the voltage security point of view, and then to alleviate the power flow across that branch in order to enhance voltage security conditions.

The technique involves, at each iteration, the utilisation of three major computational tools in sequence. Firstly, nodal voltage security assessment is performed and the weakest bus is selected; secondly, the most loaded transmission path is identified and its critical branch; and thirdly, control actions are calculated to alleviate the power flow across the critical branch. The second iteration starts with the new operating point. The process finishes if all nodal power margins are considered to be large enough, or if it is not possible to increase them.

The sample system model used in the real time supervision and control environment of CEPEL, the Brazilian Electric Power Research Centre, is shown in Fig. 1. The system comprises 34 buses, 42 transmission lines, 12 transformers and 5 generators. Voltage levels are 750, 500 and 345 kV, All generators operate with 20 kV as nominal voltage. The 750 kV corridor between buses 4 and 13 has series and shunt compensation. Buses 25 and 26 represent a large system equivalent.

3.1. Weakest bus identification

The S34_A06 operating point is shown in Fig. 2 and is the base-case in this example. As it was obtained by successive load increases at bus 29, most probably bus 29 is the weakest bus. The assessment results are shown in Table 1. On this table, S_i is the complex power injected into the load bus, S_m is an estimate of the maximum complex power that could be injected into the bus, calculated in the operating point under analysis. Therefore, $M = (S_m - S_j)/S_m$ is the complex power margin between the amount being injected and the estimated maximum (in per unit of S_m). β is the angle between the gradient vectors ∇P and ∇Q and it has being proved that $0^\circ < \beta < 180^\circ$ in the upper part of the $V \times P$ curve, while $0^\circ > \beta > -180^\circ$ in the lower half. At the maximum, the gradient vectors are aligned and thus β is equal to 0° or $\pm 180^\circ$ [3].

Negative values of β in voltage-controlled buses indicate reverse relationship between voltage and reactive power, which may lead to voltage collapse due to the automatic action of the voltage-control device having opposite effect [7]. However, the main concern in the paper is the analysis of load buses.

As expected, bus 29 is at a critical situation: its load is 34.7 pu, whereas, the maximum estimated load is 35.7 pu. Furthermore, the angle β is 178.5° and the maximum is 180°. Therefore, bus 29 is the one which might have its power margin enlarged.

3.2. Identification of the transmission paths and the most loaded one

The direction of active power flow through the transmission network is shown in Fig. 1. It is easy to verify that the subnetwork used to transmit active power to bus 29 includes all branches except those connecting the system equivalent of buses 25 and 26 to bus 24, and also branches numbered 16 and 17 connecting bus 23 to the network (in Fig. 1, the branch numbers are inside circles). Therefore, there are several transmission routes of active power from generator buses 1, 31, 32, 33 and 34 to the load bus 29. The six most loaded transmission paths are shown in Table 2. The loading condition is defined as the bus 29 voltage magnitude and angle "distance" between the operating point under analysis and the critical one. The latter corresponds to the voltage magnitude and angle at the maximum load and is calculated by the formulas for V_l^c, θ_l^c already presented. "DELTAV" is the difference between the load voltage magnitude and the criti-

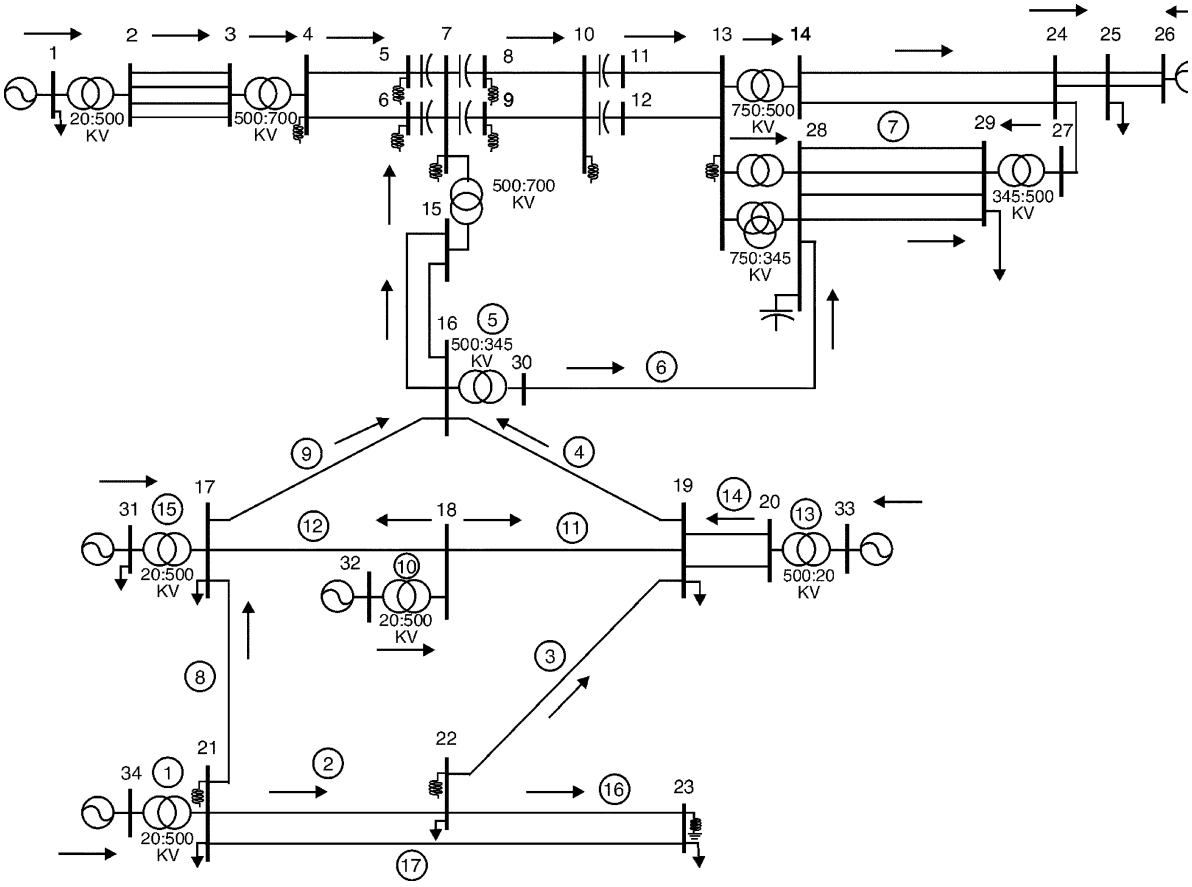

Fig. 1. 34-bus test system.

cal voltage magnitude, whereas "DELTAθ" is the difference between the load voltage angle less the critical voltage angle in radians. "DELTA$V\theta$" is a composition of those two considering orthogonal axis.

Observing Table 2 and comparing bus 29 voltage with the critical one for each transmission path, it is concluded that the six most loaded paths are shown from top to bottom starting with the most loaded path. The far right numbers order the loading.

It may be noticed in Table 2 that, taking the generator voltage as reference, both voltage drop and angular displacement are larger for the actual voltage than for the critical one, for all transmission paths. That is the reason for negative distances on the table. It may be assumed that the voltage is in the lower half of the $V \times P$ curve for all those paths.

Considering that the increase of both load and losses was supplied by generator 34, it is expected to find the most loaded paths connecting bus 29 to bus 34. And that is the case, the two

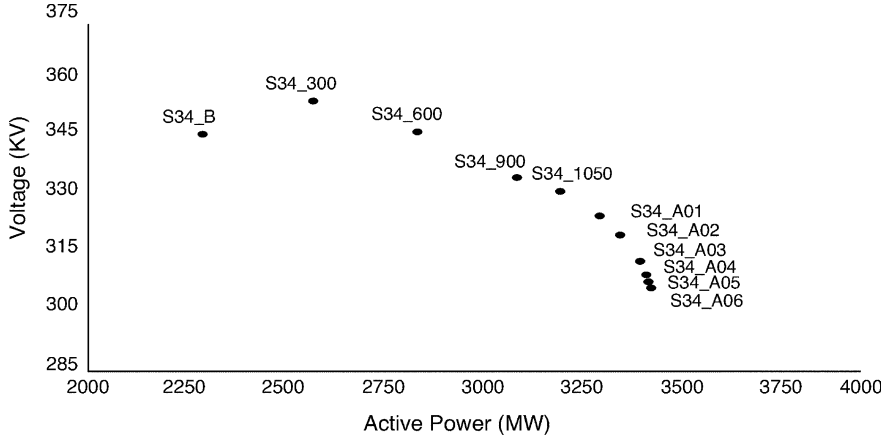

Fig. 2. Voltage magnitude vs. active power at bus 29.

Table 1
Voltage security assessment report/S34_A06 operating point

Bus number	Bus name	V (pu)	Equipment	Type	S_i (pu)	S_m (pu)	M (pu of S_m)	β (degrees)
1	BUS-001-20	1.030	GL	1	34.815	115.9	0.699	−8
2	BUS-002-500	1.012	P	0	0.000	31.6	1.000	166
3	BUS-003-500	1.010	P	0	0.000	30.7	1.000	166
4	BUS-004-750	0.951	R	0	6.279	23.3	0.730	166
5	BUS-005-750	0.916	R	0	1.374	15.5	0.911	178
6	BUS-006-750	0.915	R	0	1.373	15.5	0.911	178
7	BUS-007-750	0.932	R	0	3.076	13.0	0.763	172
8	BUS-008-750	0.986	R	0	3.255	36.5	0.911	173
9	BUS-009-750	0.987	R	0	3.257	36.5	0.911	173
10	BUS-010-750	0.906	R	0	5.983	11.0	0.456	176
11	BUS-011-750	0.921	P	0	0.000	18.8	1.000	175
12	BUS-012-750	0.922	P	0	0.000	18.7	1.000	175
13	BUS-013-750	0.882	R	0	2.911	9.5	0.693	178
14	BUS-014-500	0.966	P	0	0.000	10.7	1.000	178
15	BUS-015-500	0.876	P	0	0.000	14.4	1.000	170
16	BUS-016-500	0.879	P	0	0.000	14.7	1.000	169
17	BUS-017-500	0.999	L	0	0.044	56.2	0.999	142
18	BUS-018-500	1.037	P	0	0.000	66.1	1.000	142
19	BUS-019-500	1.050	L	0	14.998	58.5	0.744	147
20	BUS-020-500	1.052	P	0	0.000	57.5	1.000	146
21	BUS-021-500	1.074	LR	0	3.223	101.7	0.968	122
22	BUS-022-500	1.075	LR	0	2.151	59.6	0.964	125
23	BUS-023-500	1.066	LR	0	7.069	35.6	0.801	122
24	BUS-024-500	1.037	P	0	0.000	19.6	1.000	179
25	BUS-025-500	1.093	L	0	66.017	81.4	0.189	179
26	BUS-026-500	1.100	G	1	41.143	62.3	0.339	−77
27	BUS-027-500	0.991	P	0	0.000	12.7	1.000	178
28	BUS-028-345	0.869	P	0	0.000	8.2	1.000	178
29	**BUS-029-345**	**0.878**	**L**	**0**	**34.707**	**35.7**	**0.028**	**179**
30	BUS-030-345	0.929	P	0	0.000	10.5	1.000	168
31	BUS-031-20	1.007	GL	1	13.259	28.5	0.535	−39
32	BUS-032-20	1.058	G	1	12.690	25.8	0.508	123
33	BUS-033-20	1.059	G	1	12.918	14.4	0.103	−155
34[a]	BUS-034-20	1.049	G	2	14.973	–	–	–

G, generator; L, load; R, reactor; C, capacitor; P, nothing connected; 2 swing; 1, PV; 0, PQ.
[a] In order to analyse this bus, it would be necessary to select another swing bus, which is not done for simplicity.

most loaded paths connect those two buses. The following two paths connect bus 29 to generator 32, the following one to generator 33, and the last to generator 31. It is no surprise that generator 1 is not mentioned as its active power contribution to bus 29 does not use the same subnetwork used by the other generators.

3.3. Recognition of the critical branch

The objective is to determine the critical branch of the most loaded path, i.e. the branch to have its flow decreased. The idea is to examine the routes starting at generator 34, including one branch at a time. Therefore, the first path to be looked at is from bus 34 to bus 21 which comprises only branch 1. Again, the voltage at this bus is compared with the critical one corresponding to the maximum power flow arriving at this bus. Looking at Table 3 it is concluded that the bus 21 actual voltage is at the upper half of the $V \times P$ curve and far away from the critical one. Following the analysis, a new branch is included and, consequently, the second path is from bus 34 to bus 21 and to bus 22 now comprising branches 1 and 2. Again, there is no problem in transmitting power to bus 22 since its voltage presents less drop and displacement than the critical one, taking the generator voltage as reference. New branches are included sequentially and the seventh and last path includes branch from bus 28 to bus 29 and is composed of branches 1, 2, 3, 4, 5, 6 and 7. The voltage comparison indicates negative distances.

The far right numbers order the loading of the paths in Table 3. The loading condition is defined as the path terminal bus voltage magnitude and angle "distance" between the operating point under analysis and the critical one corresponding to the maximum load, the late calculated by the formulas for V_l^c, θ_l^c already presented.

Comparing the distances for all seven paths, it is concluded that there was no problem in transmitting power from generator 34 to buses 21, 22, 19, 16, 30, 28. However, there was problem in doing so for bus 29. The conclusion is that the critical branch was the last to be included, the branch 7 connecting bus 28 to 29.

Table 2
Most loaded transmission paths report/S34_A06 operating point

(magnitude in pu; angle in degrees; delta V in pu; delta θ in rd)

*** TRANSMISSION PATH: BRANCHES 7, 6, 5, 4, 3, 2, 1

	MAGNITUDE	ANGLE		
GENERATOR VOLTAGE	1.0490	22.3000		
LOAD VOLTAGE	.8829	-62.7739		
LOAD CRITICAL VOLTAGE	2.4792	9.3164		
	DELTA V	DELTA θ	DELTA Vθ	
DISTANCE	-1.5963	-1.2582	**-2.0325**	**1**

*** TRANSMISSION PATH: BRANCHES 7, 6, 5, 9, 8, 1

	MAGNITUDE	ANGLE		
GENERATOR VOLTAGE	1.0490	22.3000		
LOAD VOLTAGE	.8829	-62.7739		
LOAD CRITICAL VOLTAGE	2.3885	5.2298		
	DELTA V	DELTA θ	DELTA Vθ	
DISTANCE	-1.5056	-1.1869	**-1.9171**	**2**

*** TRANSMISSION PATH: BRANCHES 7, 6, 5, 4, 11, 10

	MAGNITUDE	ANGLE		
GENERATOR VOLTAGE	1.0580	16.7149		
LOAD VOLTAGE	.8829	-62.7739		
LOAD CRITICAL VOLTAGE	2.0906	-.7200		
	DELTA V	DELTA θ	DELTA Vθ	
DISTANCE	-1.2077	-1.0830	**-1.6222**	**3**

*** TRANSMISSION PATH: BRANCHES 7, 6, 5, 9, 12, 10

	MAGNITUDE	ANGLE		
GENERATOR VOLTAGE	1.0580	16.7149		
LOAD VOLTAGE	.8829	-62.7739		
LOAD CRITICAL VOLTAGE	2.0315	-1.7075		
	DELTA V	DELTA θ	DELTA Vθ	
DISTANCE	-1.1485	-1.0658	**-1.5669**	**4**

*** TRANSMISSION PATH: BRANCHES 7, 6, 5, 4, 14, 13

	MAGNITUDE	ANGLE		
GENERATOR VOLTAGE	1.0590	12.7291		
LOAD VOLTAGE	.8829	-62.7739		
LOAD CRITICAL VOLTAGE	1.9102	-3.5530		
	DELTA V	DELTA θ	DELTA Vθ	
DISTANCE	-1.0273	-1.0336	**-1.4573**	**5**

*** TRANSMISSION PATH: BRANCHES 7, 6, 5, 9, 15

	MAGNITUDE	ANGLE		
GENERATOR VOLTAGE	1.0070	18.1189		
LOAD VOLTAGE	.8829	-62.7739		
LOAD CRITICAL VOLTAGE	1.8863	-4.1377		
	DELTA V	DELTA θ	DELTA Vθ	
DISTANCE	-1.0034	-1.0234	**-1.4332**	**6**

3.4. Voltage security reinforcement

Bus 29 was identified as the one with a voltage security problem. The cause was ascribed to the excessive power flow across branch 7 between buses 28 and 29. Therefore, the voltage security improvement may be achieved by decreasing the power flow across that branch. The next step is to identify the most influential control variables, such as active generation and voltage set points, on the branch power flow, as well as the direction of movement of those variables. This is straightforwardly achieved by an optimal power flow (OPF) algorithm. An alternative for the OPF is to identify the contribution of each generator for the power flow in the critical branch. This may be achieved by the "upstream-looking" algorithm [4]. Redispatch is manually performed according to the sensitivities of generator output versus branch power flow. Another similar alternative is an extension of the algorithm described in [8].

Applying the control actions calculated by an OPF program [9], the new generation at the swing bus as well as the reduction of losses are shown in Table 4. The resulting voltage profile rests between 0.90 and 1.1 pu. Active power generation changes were not allowed at this first iteration, except for the swing bus responsible for absorbing the loss variations due voltage level changes.

Voltage security is assessed in the new operating point. Results are shown in Table 5. A substantial power margin $M = (1 - S_i/S_m)$ increase from 0.028 to 0.141 may be noticed. The Influence Index also translates the benefits $\mathrm{II} = (M_i/M_0 - 1) = 4.04$ or 404%. Another way to assess the

Table 3
Branch analysis of the most loaded path/S34A06 operating point

***	TRANSMISSION PATH:	BRANCH 1			
		MAGNITUDE	ANGLE		
	GENERATOR VOLTAGE	1.0490	22.3000		
	LOAD VOLTAGE	1.0752	13.5456		
	LOAD CRITICAL VOLTAGE	0.7004	-19.2129		
		DELTA V	DELTA θ	DELTA Vθ	
	DISTANCE	0.3748	0.5717	**0.6836**	**6**
***	TRANSMISSION PATH:	BRANCHES 1, 2			
		MAGNITUDE	ANGLE		
	GENERATOR VOLTAGE	1.0490	22.3000		
	LOAD VOLTAGE	1.0765	9.3915		
	LOAD CRITICAL VOLTAGE	0.6817	-24.4801		
		DELTA V	DELTA θ	DELTA Vθ	
	DISTANCE	0.3947	0.5912	**0.7108**	**7**
***	TRANSMISSION PATH:	BRANCHES 1, 2, 3			
		MAGNITUDE	ANGLE		
	GENERATOR VOLTAGE	1.0490	22.3000		
	LOAD VOLTAGE	1.0510	5.4450		
	LOAD CRITICAL VOLTAGE	0.5319	-11.6224		
		DELTA V	DELTA θ	DELTA Vθ	
	DISTANCE	0.5191	0.2979	**0.5985**	**5**
***	TRANSMISSION PATH:	BRANCHES 1, 2, 3, 4			
		MAGNITUDE	ANGLE		
	GENERATOR VOLTAGE	1.0490	22.3000		
	LOAD VOLTAGE	0.8834	-11.9938		
	LOAD CRITICAL VOLTAGE	0.8313	-1.3051		
		DELTA V	DELTA θ	DELTA Vθ	
	DISTANCE	0.0521	-0.1866	**0.1937**	**2**
***	TRANSMISSION PATH:	BRANCHES 1, 2, 3, 4, 5			
		MAGNITUDE	ANGLE		
	GENERATOR VOLTAGE	1.0490	22.3000		
	LOAD VOLTAGE	0.9341	-16.2072		
	LOAD CRITICAL VOLTAGE	0.4395	-22.2800		
		DELTA V	DELTA θ	DELTA Vθ	
	DISTANCE	0.4946	0.1060	**0.5058**	**4**
***	TRANSMISSION PATH:	BRANCHES 1, 2, 3, 4, 5, 6			
		MAGNITUDE	ANGLE		
	GENERATOR VOLTAGE	1.0490	22.3000		
	LOAD VOLTAGE	0.8739	-57.7082		
	LOAD CRITICAL VOLTAGE	0.8527	-37.4442		
		DELTA V	DELTA θ	DELTA Vθ	
	DISTANCE	0.0213	-0.3537	**0.3543**	**3**
***	TRANSMISSION PATH:	BRANCHES 1, 2, 3, 4, 5, 6, 7			
		MAGNITUDE	ANGLE		
	GENERATOR VOLTAGE	1.0490	22.3000		
	LOAD VOLTAGE	0.8829	-62.7518		
	LOAD CRITICAL VOLTAGE	2.4763	9.3134		
		DELTA V	DELTA θ	DELTA Vθ	
	DISTANCE	-1.5934	-1.2578	**-2.0300**	**1**

consequences is to compare the increase on S_m from 35.7 to 40.4 MVA, i.e. a 13% increase. Angle β decreased, as desired, from 179° to 170°. These figures indicate that reinforcement was remarkable especially if it is remembered that the base-case operating point S34_A06 was the point of collapse, as shown in Fig. 2.

At this point, the first iteration is finished. If all the nodal power margins are acceptable, the full procedure also finishes (whether the margin is acceptable or not is a question of engineering experience with the system and has not been dealt with theoretically). Otherwise, other control actions need to be calculated, this time enabling active power redispatch. Then second iteration starts.

3.5. Other reinforcement iterations

Considering the acquired experience with several tests, not shown in this paper, it was verified that better results are obtained by restricting the OPF algorithm latitude. This can be achieved by imposing fictitious limits on active generation,

Table 4
Active power generation and losses before and after decreasing branch 7 power flow

Iteration number	Active generation (MW)						Losses (MW)
	G1	G26	G31	G32	G33	G34	
S34_A06	3300	3879	1320	1200	1200	1434	604
1	3300	3879	1320	1200	1200	1385	555

Table 5
Bus 29 assessment report before and after decreasing branch 7 power flow

Iteration number	V (pu)	S_i (pu)	S_m (pu)	M (pu of S_m)	β (degrees)
S34_A06	0.878	34.707	35.7	0.028	179
1	0.908	34.707	40.4	0.141	170

say ±10% around the actual active power generation values (if ficticious limits remain inside actual limits). Although, not mandatory, the exception is the swing bus responsible for closing the active balance.

If constraining limits were not adopted, the OPF algorithm would minimise the power flow as much as possible, even reversing the flow direction. And that is not the goal, which is only to alleviate the flow in order to enlarge the power margin at the weakest bus.

The most loaded transmission paths and their critical branches are shown in Table 6 for seven strengthening iterations. The active power generations and the losses are shown in Table 7. It is to be noticed that after the sixth iteration, generation at bus 34 and the losses start to increase in opposition to what was observed in the first six iterations. The voltage security assessment results for bus 29 are shown in Table 8 for all seven iterations. The assessment was carried out at each operating point after enhancement control actions have been applied.

Table 6
Weakest bus, most loaded path and critical branch before each reinforcement iteration

Iteration	Weakest bus	Most loaded transmission path	Critical branch
1	29	Branches 1, 2, 3, 4, 5, 6, 7	7
2	29	Branches 1, 2, 3, 4, 5, 6, 7	7
3	29	Branches 15, 8, 2, 3, 4, 5, 6, 7	7
4	29	Branches 10, 11, 4, 5, 6, 7	7
5	29	Branches 10, 11, 4, 5, 6, 7	7
6	29	Branches 15, 12, 11, 4, 5, 6, 7	7
7	29	Branches 15, 12, 11, 4, 5, 6, 7	12

Table 7
Active power generation and losses after each reinforcement iteration

Iteration	Active generation (MW)						Losses (MW)
	G1	G26	G31	G32	G33	G34	
S34_A06	3300	3879	1320	1200	1200	1434	604
1	3300	3879	1320	1200	1200	1385	550
2	3618	4267	1307	1192	1196	634	481
3	3967	4694	1212	1108	1111	41	400
4	3765	5163	1101	1007	1009	9	320
5	3473	5679	999	914	915	7	253
6	3128	6247	900	824	825	1	192
7	3390	5921	810	906	908	3	204

Table 8
Bus 29 voltage security assessment report after each reinforcement iteration

Iteration	V (pu)	S_i (pu)	S_m (pu)	M (pu of S_m)	β (degrees)
S34_A06	0.878	34.707	35.7	0.028	179
1	0.908	34.707	40.4	0.141	170
2	0.906	34.707	43.4	0.200	165
3	0.907	34.707	47.0	0.261	155
4	0.948	34.707	51.2	0.322	141
5	0.964	34.707	54.1	0.358	131
6	0.996	34.707	57.9	0.401	119
7	0.997	34.707	61.1	0.432	121

The operating point after reinforcement iteration number 7 was assessed and bus 29 was the weakest one once again. The most loaded transmission path and the critical branch were determined. The OPF algorithm was applied but unsuccessfully, it was not possible to increase the bus 29 power margin. Probably, because bus 34 active power generation reached its minimum value interrupting the trend noticed in the iterations before. Therefore, the operating point after seven iterations is considered the best possible. As a matter of fact, bus 29 power margin $M = (1 - S_i/S_m)$ was significantly increased, from 0.028 to 0.432 pu of S_m. The Influence Index translates the benefit:

$$\mathrm{II} = \left[\left(\frac{M_i}{M_0}\right) - 1\right] = 14.43 \text{ or } 1443\%.$$

The figure is quite big because the initial margin M_0 is too small since the S34_A06 operating point is almost at the maximum load.

Another numerical assessment of the control action consequences is to verify that S_m increased from 35.7 to 61.1 pu, which means an improvement of 71%. Concurrently, angle β decreased, as desired, from a quite critical value of 179° to 121°.

The method was successfully applied to several systems including the IEEE 24 buses, the Brazilian S/SE equivalent system with 395 buses, and the full S/SE system with 1750 buses. It should be noticed that the problem size does not increase with the number of system buses. In order to justify this statement, consider that the system equivalent represented by buses 25 and 26 in the unifilar diagram of Fig. 1 is now fully represent with, say, 100 buses, 130 branches and 10 generators. However, none of those buses, branches and generators participate in the problem of the numerical example (since active power flows from bus 24 to that system). In other words, only a small region of a very large network is used to transmit power to a load area with constrained transmission due to voltage stability problems. In the numerical example, the load area is represented by bus 29 and the constrained network comprises buses 34, 21, 22, 19, 16, 30, 28, 29, 17, 32, 18, 33, 20, 31 and branches 1, 2, 3, 4, 5, 6, 7, 8,

9, 10, 11, 12, 13, 14, 15. The other 20 buses and 42 branches are not involved in the problem. Another argument to justify that the problem size does not increase with the number of system buses is quite commonly found in the literature; voltage stability problem is associated with lack of local reactive power support and the latter is usually confined into an area of the network.

In the numerical example with the 34-bus system shown in this paper, the problem was artificially created by increasing bus 29 load followed by increasing bus 34 generation. In other tests where load and generation increase are spread in several buses; the weakest bus, the most loaded transmission path and the critical branch vary from one iteration to another during the margin enhancement procedure.

4. Comparison with similar techniques

Although there are hundreds of papers in the literature about voltage security assessment, there are only about 10 on voltage security reinforcement. None of them seems to be useful for operational purposes. The most similar technique is based on the modal analysis of the $[\partial P/\partial\theta]$ matrix, a partition of the power flow Jacobian matrix [10]. Right and left eigenvectors are calculated for the smallest eigenvalue in order to build up the participation factors. Generators with large factors are to have its output decreased while those with small factors are to have its output increased. No reinforcement is possible when all generator factors are about the same size.

Modal analysis based on the calculation of "small eigenvalues" [11] or "small singular values" [12], although adequate for expansion planning studies, has never being recommended for operational purposes. The establishment of voltage stability indices representing the instantaneous margin of the current operating point with respect to the instability limit should be the objective for real-time analysis [13]. These indices should be necessarily based on real-time measurements of the network and its controls, and has to be computed in a short time (few seconds).

The modal analysis presents a number of drawbacks when applied to operational studies. In the context of this paper, it may be stated that there is no way to compare voltage security robustness between two operating points, such as before and after a control action is applied. It may also be said that a null eigenvalue does not correspond to maximum power transmission to a load bus, if power flow equations include the modelling of special equipments (DC link, SVC, TSSC, etc.), controls (voltage, power interchange, etc.) and limits.

This is the first paper that, in order to calculate enhancement control actions, deals with the origin of the voltage security problem: the excessive power flow across a certain transmission branch. Furthermore, in order to verify the adequacy of the control actions, the actual physical variable of interest is monitored: the power margin.

5. Conclusions

An iterative and sequential technique for voltage security reinforcement was presented. The task involved the utilisation of three different computational tools. The first one carries out the nodal voltage security assessment and points out the weakest bus. The second tool determines the transmission paths used to carry active power from generators to the weakest bus and, among them, selects the most loaded one. The critical branch of the most loaded transmission path is determined. The third tool, an OPF algorithm, is used to alleviate the power flow across the critical branch by performing voltage profile adjustments and, if necessary, active generation redispatch.

The technique was successfully applied to several systems and operating points. The computational time does not increase with system size and is no burden for real time applications.

Acknowledgements

This paper presents partial results of research contracts AE 16/98 and CON 02/01 between FPLF of PUC/Rio and CEPEL. The first two authors received financial support from CNPq and FAPERJ.

References

[1] R.B. Prada, B.J. Cory, R. Navarro-Perez, Assessment of steady state voltage collapse critical conditions, in: 10th Power Systems Computation Conference, Graz, Austria, 1990, pp. 1189–1195.
[2] R.B. Prada, A.C. Zambroni, X. Vieira Filho, A.G. Massaud, J.C.C. Oliveira, Voltage stability: phenomena characterisation based on reactive control effects and system critical areas identification, in: III Symposium of Specialists in Electric Operational and Expansion Planning, Belo Horizonte, Brazil, 1992.
[3] R.B. Prada, E.G.C. Palomino, J.O.R. Dos Santos, A. Bianco, L.A.S. Pilotto, Voltage stability assessment for real time operation, Proc. IEE Generation Transm. Distribution 149 (2) (2002) 175–180.
[4] J. Bialek, Tracing the flow of electricity, Proc. IEE Generation Transm. Distribution 143 (4) (1996) 313–320.
[5] E.W. Kimbark, Power System Stability, Synchronous Machines, vol. III, Dover Publications, 1968.
[6] H.E. Brown, R.B. Shipley, D. Coleman, R.E. Neid Jr., A study of stability equivalents, IEEE Trans. Power Apparatus Syst. 88 (1) (1969) 200–207.
[7] R.B. Prada, L.J. Souza, L.A.P. Sousa, The need for a new constraint on voltage/reactive power studies to ensure proper voltage control, Int. J. Electrical Power Energy Syst. 24 (June (7)) (2002) 535–540.
[8] R.M. Silva, L.D.B. Terra, Market power under transmission congestion constraints, in: IEEE Powertech Conference, Budapest, Hungary, 1999, paper BPT99-121.
[9] S. Granville, Optimal reactive dispatch through interior point methods, IEEE Trans. Power Syst. 9 (1) (1994) 136–146.
[10] L.C.P. da Silva, Y. Wang, V.F. da Costa, W. Xu, Assessment of generator impact on system power transfer capability using modal

participation factors, Proc. IEE Generation Transm. Distribution 149 (5) (2002) 564–570.
[11] B. Gao, G.K. Morison, P. Kundur, Voltage stability evaluation using modal analysis, IEEE Trans. Power Syst. 7 (4) (1992) 1529–1542.
[12] P.-A. Löf, T. Smed, G. Andersson, D.J. Hill, Fast calculation of a voltage stability index, IEEE Trans. Power Syst. 7 (1) (1992) 54–64.
[13] S. Corsi, M. Pozzi, U. Bazzi, M. Mocenigo, P. Marannino, A simple and real-time on-line voltage stability index under test in Italian secondary voltage regulation, CIGRÉ Biannual Session, Paris, France, September 2000, paper 38-115.